J Therm Anal Calorim (2009) 98:495–505
DOI 10.1007/s10973-009-0312-0

LCST demixing in poly(vinyl methyl ether)/water studied by means of a High Resolution Ultrasonic Resonator

Kurt Van Durme · Guy Van Assche · Hubert Rahier · Bruno Van Mele

Received: 8 January 2009 / Accepted: 13 January 2009 / Published online: 28 August 2009

Abstract A High Resolution Ultrasonic Resonator is applied to study demixing and remixing of poly(vinyl methyl ether) (PVME)/water solutions. The observed variation in ultrasonic properties (i.e., velocity and attenuation) is discussed in relation to microcalorimetry and Modulated Temperature DSC results. Throughout the phase separation process the ultrasonic velocity decreases due to the release of water molecules from the polymer hydration structure, while on the other hand the ultrasonic attenuation increases once aggregation sets in. The overall evolution of both ultrasonic signals is governed by the peculiar shape of the bimodal LCST demixing curve of PVME/water. The technique gives reliable results up to 20 weight% PVME.

Keywords Poly(vinyl methyl ether) · Phase separation · High Resolution Ultrasonic Resonator · Hydrophilic polymer · Bimodal LCST

Introduction

High Resolution Ultrasonic Spectroscopy (HR-US) is a non-destructive analytical tool based on precision measurements of properties of (low energy) ultrasonic waves propagating through a sample. The produced oscillating pressure causes mechanical deformation of the studied material, i.e., compression in the ultrasonic wave changes the intermolecular distances in the sample, to which the molecules respond by intermolecular repulsions, causing them to return to their original positions. The propagation of a sound wave thus depends on the transfer of vibrations from one molecule to another. Therefore, ultrasonic spectroscopy enables direct probing of the intermolecular forces in the analyzed medium and thus the analysis of its physical and chemical properties [1–4].

The propagation of ultrasonic waves is essentially characterized by the velocity (U) and the attenuation. In liquids, the former is related to the density ρ and the elastic properties of the sample that can be expressed in terms of adiabatic compressibility β_S (Eq. 1).

$$U = \frac{1}{\sqrt{\beta_S \rho}} \tag{1}$$

The velocity change that results from molecular rearrangements is mainly governed by variations in compressibility [5, 6]. As a result, sound waves travel faster in solids than they do in liquids and gases, because solids contain the strongest molecular interactions (small compressibility) followed by liquids and gases (larger compressibility). The ultrasonic velocity is extremely sensitive to intermolecular interactions, molecular organization and composition of the analyzed medium [2, 3, 7–10]. The ultrasonic attenuation originates from energy losses during consecutive compressions and decompressions in ultrasonic waves. In a regular liquid, these energy losses can be described by the mechanism of viscous damping and heat conduction [11]. Additionally, in binary polymer solutions showing critical solution behavior, the alternating adiabatic compression and expansion of the fluid generate a change in the local temperature and the pressure dependent critical temperature. Due to the lagged response of the concentration fluctuations energy is dissipated, adding up to the ultrasonic attenuation value [12–14]. There exist several

K. Van Durme · G. Van Assche · H. Rahier · B. Van Mele (✉)
Vrije Universiteit Brussel (VUB), Faculty of Engineering, Physical Chemistry and Polymer Science – MACH\FYSC, Pleinlaan 2, 1050 Brussels, Belgium
e-mail: bvmele@vub.ac.be

theories, which describe the correlation between critical fluctuations and the resulting excess ultrasonic attenuation, either linked to a frequency-dependent complex heat capacity or viscosity [15–17]. These theories have been refined many times and will not be discussed in detail here. Additionally, non-homogeneous samples may exhibit scattering of the ultrasonic waves, which is a major factor contributing to the attenuation value [2, 4]. In the long wavelength limit (if particle size is much smaller than the applied wavelength), two major scattering aspects can be distinguished, i.e., viscoinertial and thermoelastic [18].

Ultrasonic characterization of various molecular properties, such as hydration, structural characterization of colloid systems, molecular organization, composition analysis, and crystallization was performed in the last decades [18–28]. In most of these measurements, a pulse (or an equivalent excitation) technique was used, of which the resolution in measuring the ultrasonic parameters is determined by the path length of the pulse and thus by the size of the sample [23]. This limited the application of ultrasonic spectroscopy to concentrated systems and to molecular processes, which are accompanied by a large change in ultrasonic parameters. Recently commercialized High Resolution Ultrasonic Resonators, however, employ novel principles, enabling deconvolution of the sample size and thus enhancing the resolution of the acoustic measurement [1, 2]. In this technique, a piezotransducer excites the ultrasonic wave traveling through the sample toward the second piezotransducer. Being reflected by the second piezotransducer the wave comes back and is reflected again. At certain frequencies a resonance occurs causing an increase in the amplitude of the signal. The ultrasonic parameters (i.e., velocity and attenuation) are calculated based upon the resonance characteristics of which a more elaborated discussion can be found in literature [1].

This work focuses on the potential applicability of HR-US to study the phase behavior of poly(vinyl methyl ether) (PVME) in water. PVME is a hydrophilic polymer that separates from aqueous solution upon heating. The observed demixing process results from small temperature-dependent changes of inter- and intramolecular interactions, i.e., a varying competition between hydrogen bonding and hydrophobic interactions [29–31]. At low temperatures, the accessible hydrophilic ether oxygens stabilize the homogeneous aqueous solution. Hence, the attained water-structure surrounding the polymer chains prevents the hydrophobic groups from coming together [32]. However, at elevated temperatures the ordered hydration structure is destroyed, resulting in aggregation of the polymer chains due to hydrophobic associations. This is accompanied by an endothermic heat effect and a rising opacity of the PVME/water solution [33–36]. The PVME/water system is characterized by a type III LCST miscibility behavior that consists of a bimodal demixing curve of which the critical concentrations show a different molar mass dependence [33, 37, 38]. That is, the critical concentration in the low concentration range shifts toward lower temperature and concentration with increasing polymer molar mass as expected from the classical Flory–Huggins miscibility behavior, whereas the one at high PVME concentration is nearly molar mass independent [36]. The intersection of both two-phase areas defines an invariant three-phase equilibrium at constant temperature. A more general description of type III LCST demixing behavior can be found in the work of Schäfer-Soenen et al. [37].

Throughout this paper HR-US will be evaluated for studying the phase behavior of PVME/water mixtures nearly spanning the entire composition range. The HR-US results will be compared with data obtained by microcalorimetry and Modulated Temperature Differential Scanning Calorimetry (MTDSC). In both techniques, the heat effect of both phase separation and remixing is used to study the transformation. Microcalorimetry is commonly used to study phase separation of dilute (aqueous) polymer solutions (e.g., [39–41]), although studies over the full concentration range are rare.

Through the simultaneous measurement of heat flow and heat capacity, MTDSC is a powerful tool for the characterization of demixing and remixing in polymer solutions and partially miscible polymer blends [33, 42–44]. A comprehensive description of the extraction of the heat capacity and other MTDSC signals can be found in literature [45, 46]. In the study of polymeric materials using MTDSC, kinetic thermal processes depending on time and absolute temperature, appear in the non-reversing heat flow, while the (specific) heat capacity appears in the reversing heat flow. This straightforward deconvolution procedure turns out to be valid for the study of many reacting polymer systems [47]. However, it no longer holds when characterizing polymer melting [48] or temperature-induced phase separation in polymer solutions and blends [33, 42–44]. Heat effects, coupled with melting/crystallization or mixing/demixing, occur during one modulation cycle and thus contribute to the amplitude of the modulated heat flow causing an excess contribution in the heat capacity signal. By performing a time domain analysis of the modulated heat flow [33, 43], the enthalpic origin of c_p^{excess} could be established, i.e., raising the temperature within one modulation cycle causes an endothermic excess heat effect (coupled with demixing), while cooling within the same modulation cycle generates an equivalent exothermic heat effect (coupled with remixing). Because of the occurrence of this excess contribution, c_p^{excess}, originating from fast enthalpic (reversible) processes, the observed specific heat capacity is termed apparent specific heat

capacity, c_p^{app}, to distinguish it from the baseline specific heat capacity, c_p^{base}.

$$c_p^{app}(T,t) = c_p^{base}(T) + c_p^{excess}(T,t) \quad (2)$$

c_p^{base} is (to a good approximation) only temperature-dependent. c_p^{excess} is temperature- and time-dependent and changes with the progress of the transformation (slow process). Indeed, the observed slow evolution in c_p^{excess}, and thus c_p^{app}, can be linked to macroscopic morphological changes reflecting the associated interphase development, as already explored in previous work on aqueous polymer systems [33, 42, 43]. In that case, the observed time dependency was related to the diffusion of water molecules inside the polymer aggregates together with the specific interactions of these water molecules adjacent the polymer chains until an equilibrium situation is reached. The varying c_p^{excess}-value reflects the varying sample fraction participating in the exchange process at the polymer/water interphase of the coexisting phases. Note that by choosing the appropriate modulation conditions, i.e., amplitude and period, the reversible demixing/remixing process at the polymer/water interphase is fast enough to attain a frequency-independent excess contribution in the apparent heat capacity signal.

Experimental

Preparation of polymer/water solutions

PVME (dissolved in water, 50/50 wt/wt) was purchased from Aldrich Chemical Company Inc. (weight average molecular weight, $M_w = 20{,}000$ g mol^{-1} and polydispersity, $M_w/M_n \sim 2.5$ derived from Gel Permeation Chromatography). The polymer was dried under vacuum for at least 48 h at 40 °C, until the water content was less than 0.2 wt% as determined by Thermo Gravimetric Analysis (TA Instruments TGA 2950). The glass transition temperature (T_g) of dried PVME equals −25 °C [49].

A range of compositions (wt/wt) was prepared, by adding the appropriate amount of water to dried PVME, after which the samples were stored in the refrigerator for at least one month to obtain a homogeneous mixture.

High Resolution Ultrasonic Spectroscopy

High Resolution Ultrasonic Spectroscopy (HR-US) measurements were performed on a HR-US 102 resonator (Ultrasonic Scientific) fitted with two 1 mL cells. The principles of the measurement of ultrasonic velocity and attenuation, employed in this method, are described earlier [1]. All experiments were done at selected frequencies (*f*): 7.5, 11.6 and 14.6 MHz. The cells were filled with 1 mL of water (reference) and polymer/water solution, respectively. The limiting resolution for the ultrasonic velocity is 0.2 mm s^{-1} and 0.2% for the ultrasonic attenuation. Non-isothermal experiments were carried out at standard heating/cooling rates of 0.2 °C min^{-1}. The demixing temperature upon heating was determined using a threshold value of 0.01 m s^{-1}, defined against the extrapolated experimental ultrasonic velocity of the homogeneous sample.

Microcalorimetry

Microcalorimetry measurements were performed on a Thermal Activity Monitor TAM-III (Thermometric, Sweden) with 6 Minicalorimeters (type 3206, 4 mL) in a Multicalorimetric unit (type 3208) positioned in an access bay of the TAM III Thermostat (type 3101). Non-isothermal experiments were performed at a heating rate of 2 °C h^{-1} between 20 and 60 °C after stabilizing for one day at 20 °C. Since the scanning rate is very low, the sample can be considered to be in virtual thermal, chemical, and physical equilibrium during the measurement. The sample heat flow is obtained by subtracting the response measured for empty glass ampoules from the response of the sample (measured in the same minicalorimeter). It can be expressed as a heat capacity by division through the heating rate. A heat capacity calibration was performed using Millipore Milli-Q water as a calibrant.

The demixing temperature upon heating was obtained using a threshold value of 0.05 J g^{-1} K^{-1} against the extrapolated experimental baseline heat capacity, obtained by fitting a second order polynomial versus temperature over a temperature interval of at least 10 °C (correlation coefficients larger than 0.998).

Modulated Temperature Differential Scanning Calorimetry

Modulated Temperature Differential Scanning Calorimetry (MTDSC) measurements were performed on a TA Instruments 2920 DSC with the MDSC^{TM} option and a refrigerated cooling system (RCS). Helium was used as a purge gas (25 mL min^{-1}). Indium and cyclohexane were used for temperature calibration. The former was also used for enthalpy calibration. Heat capacity calibration was performed using Millipore Milli-Q water, at 20 °C. Data are expressed as specific heat capacities (or changes) in J g^{-1} K^{-1}.

Samples of 1–5 mg were introduced in Mettler aluminum pans that were subsequently hermetically sealed. Non-isothermal experiments were performed at an underlying heating/cooling rate of 0.2 °C min^{-1}. Standard modulation

conditions were an amplitude of 0.50 °C with a period of 60 s. The demixing temperature upon heating was obtained using the same procedure as for the TAM measurements. At higher temperatures the apparent heat capacity becomes time-dependent (see introduction), illustrating the ongoing phase separation process.

Light Scattering

Cloud points were determined by measuring the light transmitted through thin samples between glass slides mounted in a Mettler Toledo FP82HT hot stage, which was placed in a Spectratech optical microscope (magnification 10×) equipped with a photo detector (most sensitive at a wavelength of 615 nm). Temperature calibration was done with benzophenone. All samples were heated (and cooled) at 0.2 °C min^{-1}. A threshold value of 2% in the decrease of light transmittance (against 100% for the transparent homogeneous solution) upon heating was chosen as the cloud point temperature.

Results and discussion

The ability for studying the phase behavior of PVME/water solutions using a High Resolution Ultrasonic Resonator is explored, and the ultrasonic data are discussed in relation to results from Microcalorimetry, Modulated Temperature DSC, and Light Scattering.

Non-isothermal demixing

Figure 1 shows the temperature-dependence of the ultrasonic velocity in pure water and in an aqueous PVME solution. In a regular liquid the speed of sound decreases with temperature, but in water it increases (Fig. 1, filled circle) up to 74 °C, demonstrating its atypical behavior [50]. The observed increase of the velocity of water with temperature is related to a change in its unique structure. That is, at low temperatures both compressibility and density are high, causing a low speed of sound (see Eq. 1). As the temperature increases the compressibility decreases and goes through a minimum at 46 °C, while the density goes through a maximum at 4 °C [51]. The combination of both properties leads to the anomalous maximum in the speed of sound [52].

In Fig. 1, a similar increase of the ultrasonic velocity is noticed upon heating a 1/99 PVME/water mixture (open circle), although the absolute value is higher. This results from the lower compressibility of the polymer/water mixture with respect to pure water. Shinyashiki et al. revealed, by dielectric studies, that the mobility of water molecules near PVME chains is highly reduced as they are

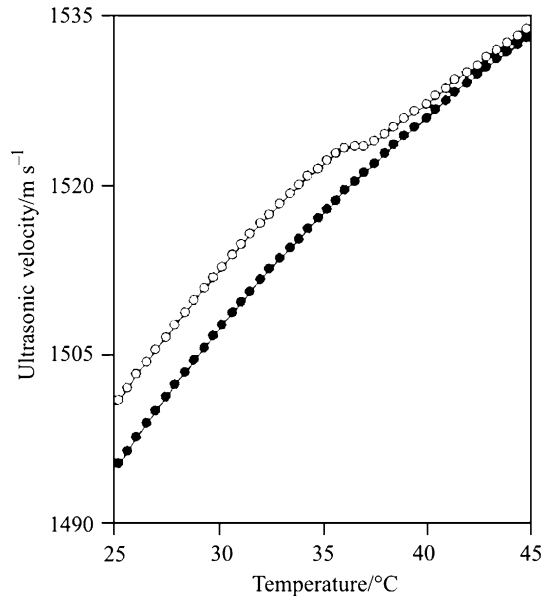

Fig. 1 Ultrasonic velocity of water (*filled circle*) and of 1/99 PVME/water (*open circle*) upon heating

incorporated in the polymer hydration sheath [53–55]. The resulting restricted mobility consequently causes a substantial decrease in compressibility and thus a higher ultrasonic velocity.

At a certain temperature (ca. 33.5 °C), a gradual deviation is noticed, caused by the phase separation process, which reflects the change in polymer hydration structure and in the compressibility of the formed polymer aggregates. Below the demixing temperature (T_{demix}) the PVME/water mixture exhibits predominantly intermolecular hydrogen bonding, while above T_{demix} hydrophobic interactions dominate [35]. As a result, the amount of free water will considerably augment during the demixing process. Since free water is typically more compressible than bound water [25, 26] one expects the ultrasonic velocity to decrease at T_{demix} (Fig. 1, open circle). In the following discussion, the contribution of pure water will be subtracted and the difference in velocity ($U_{sample} - U_{water}$) is used in order to analyze the details of the transition (Fig. 2a). By doing so, one can observe that the demixing process consists of two distinct steps, indicated by the vertical lines in Fig. 2. This observation is in agreement with the bimodal shape of the LCST demixing curve, i.e., the initial stages of phase separation above T_{demix} (vertical line at ca. 33.5 °C) are followed by large compositional changes upon passing the temperature at the three-phase equilibrium ($T_{3\text{-phase}}$) (vertical line at ca. 36.5 °C) [33, 37, 38, 56]. These two steps are also noticed in the ultrasonic attenuation signal (Fig. 2b) that is related to the scattering of ultrasonic waves within the sample, thus reflecting morphology changes during phase separation [4, 7]. Below T_{demix} a fairly constant attenuation level is usually

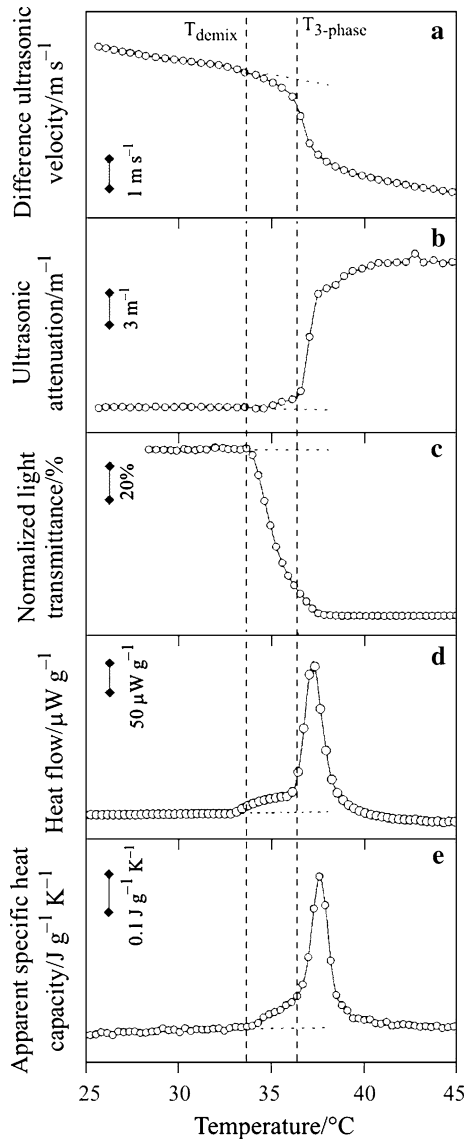

Fig. 2 Non-isothermal demixing of 1/99 PVME/water: **a** difference ultrasonic velocity (HR-US), **b** ultrasonic attenuation (HR-US), **c** normalized light transmittance (LS), **d** microcalorimetric heat flow (TAM III), and **e** apparent specific heat capacity (MTDSC). *Dashed lines* are a guide to the eye

observed, representative for the swollen (entangled) polymer coils in the aqueous solution. As soon as demixing sets in the attenuation starts to increase due to the scattering of ultrasonic waves through aggregation of the collapsed PVME chains [57]. At $T_{3\text{-phase}}$, the attenuation additionally increases caused by an abrupt change in composition. At higher temperatures (near 38.5 °C) the attenuation levels off and another nearly constant level is reached, which seems reasonable as above $T_{3\text{-phase}}$ both final co-existing phases are attained and no extra compositional changes have to occur, governed by the state diagram.

The observed two-step process when demixing a PVME/water solution (Figs. 2 and 3, open circle) relates to the bimodal shape of the special type III LCST demixing behavior. Hence, the largest variation in both ultrasonic signals occurs upon passing the temperature at the three-phase equilibrium, following the initial stages of phase separation. Conversely, phase separation of any aqueous PNIPAM solution can be described by a single transition (Fig. 3, filled circle) reflecting the type II LCST demixing curve and its interference with the T_g-composition curve, comprehensively elaborated in previous work [4, 43].

A rather good agreement is found between the start of demixing (Fig. 2, vertical line at ca. 33.5 °C) using HR-US, the decrease in the normalized light transmittance (LS: Fig. 2c), the initial deviation of the heat flow from the baseline in microcalorimetry (μCal: Fig. 2d), and the initial deviation in the apparent specific heat capacity c_p^{app} (MTDSC: Fig. 2e) from the baseline heat capacity. The agreement is very good, especially when taking into account that the measurements for these dilute solutions (1 wt% PVME), in a concentration range where the onset of phase separation strongly depends on concentration, were made on individually prepared solutions.

Note that when using MTDSC (with the standard modulation conditions of 0.50 °C per 60 s) the total demixing enthalpy is separated into two endothermic contributions [33]. Usually, the largest part is found in the heat capacity signal (and correspondingly in the reversing heat

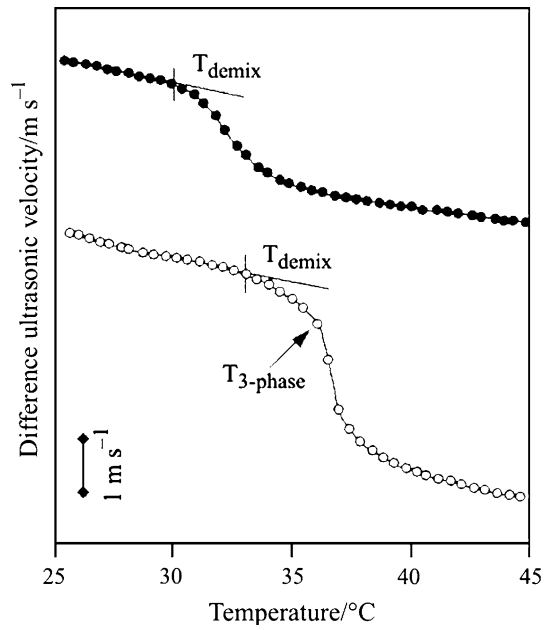

Fig. 3 Difference ultrasonic velocity during non-isothermal demixing of 1/99 PVME/water (*open circle*) and PNIPAM/water (*filled circle*) [4], curves are shifted vertically for clarity. *Lines* are a guide to the eye

flow), whereas the non-reversing heat flow contains the remaining part. Hence, the former signal is termed apparent (c_p^{app}) to distinguish it from the baseline specific heat capacity, c_p^{base}. The apparent specific heat capacity displays a broad peak that is characteristic for a type III LCST demixing behavior. A very similar peak is observed by microcalorimetry. At first, the sample is heated through a two-phase region, which is seen as a shoulder prior to a large peak, having a maximum at ca. 37 °C and caused by passing the three-phase equilibrium. On the other hand, in MTDSC a sharp (single) transition is seen in the non-reversing heat flow (not shown), occurring just before the maximum of the large peak in c_p^{app}. The onset temperature of the heat effect in the non-reversing heat flow (MTDSC), the peak maximum in c_p^{app} (MTDSC), or the peak maximum in c_p (microcalorimeter) can thus be used to determine the invariant three-phase equilibrium [33].

The temperature at the three-phase equilibrium (Fig. 2, vertical line at ca. 36.5 °C) is also in good agreement for the different analytical techniques, although usually it cannot be deduced from LS. Generally, the normalized light transmittance immediately drops to zero at T_{demix} when studying more concentrated mixtures (≥3 wt% PVME) due to a high level of aggregation, making it impossible to detect additional morphological or structural changes.

The effect of concentration on the ultrasonic (HR-US) data will be explained in following section, consequently leading to the construction of a state diagram.

State diagram of PVME/water

The evolution of the difference ultrasonic velocity (Fig. 4a) as well as the ultrasonic attenuation (Fig. 4b) is quite similar for every composition and is a reflection of the PVME/water state diagram (Fig. 5). The compositional changes in a PVME/water sample gradually start at T_{demix} and considerably enlarge at $T_{3\text{-phase}}$ up to ca. 38.5 °C, describing the formation of both a water- and PVME-rich phase (following the LCST demixing curve). The disentanglement of this two-step process is best noticed for a 10/90 PVME/water mixture (Fig. 4, filled circle), which seems quite logical as this composition is situated near the minimum of the two-phase area at low PVME concentration (Fig. 5).

In deriving the state diagram, the difference velocity was preferred over the attenuation, because the former contains less noise. Nevertheless, similar results can be obtained, since the temperature at which both signals deviate from their respective baseline differs less than 0.2 °C. When using an appropriate baseline and threshold value for each technique for the determination of the phase separation temperatures, microcalorimetry, MTDSC, and

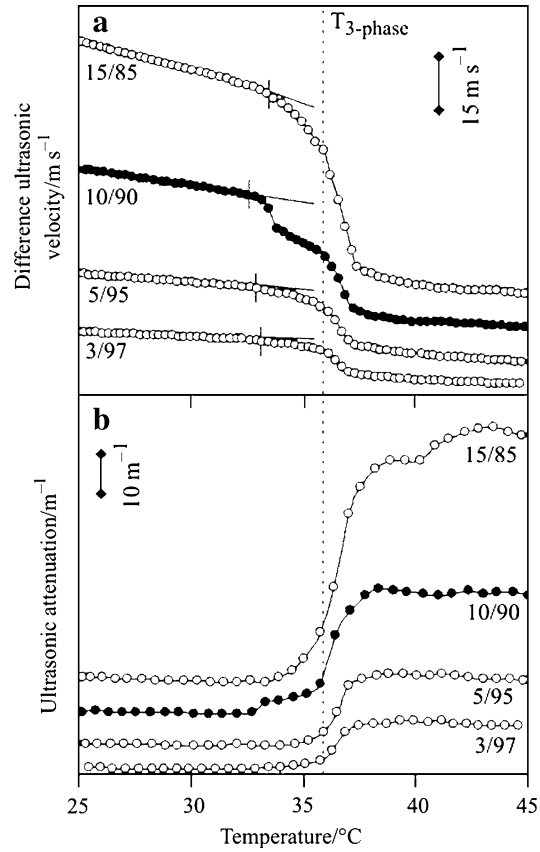

Fig. 4 Non-isothermal demixing of PVME/water for different compositions: **a** difference ultrasonic velocity, curves are shifted vertically for clarity; **b** ultrasonic attenuation ($f = 7.5$ MHz). *Lines* are a guide to the eye

LS give similar results, as well as HR-US (Fig. 5b, open square). On the other hand, the temperature at the three-phase equilibrium from MTDSC (Fig. 5a, diamond) and HR-US (Fig. 5b, dash) correspond within 1 °C.

Note that for solutions containing more than 60 wt% PVME no reproducible results with HR-US could be obtained; therefore these results were not included in the state diagram (Fig. 5b). This concentration limit depends on the algorithm used in following the change in ultrasonic parameters with temperature.

The shape of the state diagram in Fig. 5 differs somewhat from the state diagram presented in previous work [33]. These differences originate mainly from the use of a quadratic (instead of a linear) extrapolated baseline heat capacity for performing the threshold evaluation to determine the onset temperature of phase separation. Especially in the concentration range of 20–40 wt% PVME, this results in a slightly higher phase separation temperature, as illustrated in Fig. 6a for the MTDSC results. However, more important is that for the different solutions similar shapes of the phase separation event are observed by microcalorimetry and MTDSC: a stepwise onset of phase

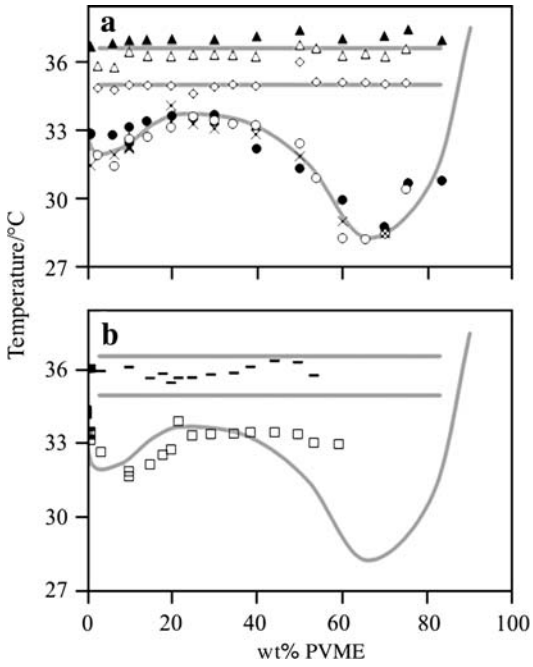

Fig. 5 State diagram of PVME/water: **a** demixing temperatures from microcalorimetry (*filled circle*), MTDSC (*open circle*), and LS (X); temperature at the three-phase equilibrium with microcalorimetry (*filled triangle*), MTDSC (onset non-reversing heat flow: *diamond*, max c_p^{app} *open triangle*); **b** demixing temperatures from HR-US (*open square*); temperature at the three-phase equilibrium with HR-US (*dash*). Gray lines are the same in (**a**) and (**b**) and serve as a guide to the eye

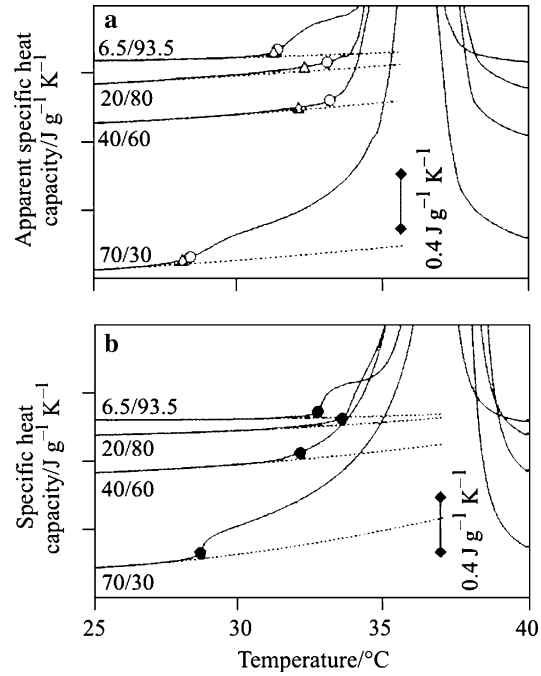

Fig. 6 Non-isothermal demixing of PVME/water for different compositions: **a** apparent specific heat capacity c_p^{app} from MTDSC and **b** specific heat capacity c_p from microcalorimetry. Demixing temperatures from microcalorimetry (*filled circle*) and MTDSC (*open circle*) calculated using a quadratic baseline (- - -); and from MTDSC (*open triangle*) using a linear baseline (threshold in all cases 0.05 J g^{-1} K^{-1})

separation followed by an increase to the maximum at higher temperature for 6.5/93.5 and 70/30, compositions close to the minima in the demixing curve, compared to a sharper onset of the main peak for 20/80 and 40/60, compositions closer to the region where the left and right lobe of the demixing curve meet. The similarity of the heat capacity evolution from microcalorimetry and the apparent heat capacity from MTDSC, measured in quite different experimental conditions (heating rate, presence modulation), indicates that the initial shape of the curve is dictated by thermodynamics (i.e., the bimodal state diagram with a three phase equilibrium) rather than a result of kinetic effects.

Concentration-, temperature- and frequency-dependence of ultrasonic properties

During phase separation the hydrated polymer coils collapse and aggregate, altering the ultrasonic properties of the PVME/water system. Based upon Fig. 4, the overall stepwise change between T_{demix} and 38.5 °C, in both velocity and attenuation can be determined. These stepwise changes (delta), denoted as delta ultrasonic velocity (Fig. 7, open circle) and delta ultrasonic attenuation (Fig. 7, filled circle), describe the degree of phase separation. (Delta) Ultrasonic velocity is related to the change in compressibility, resulting from the release of water molecules from the hydration structure surrounding the polymer chains, while delta ultrasonic attenuation is related to energy losses by scattering of the ultrasonic waves. The more and/or the larger the aggregates formed, the larger the stepwise changes expected. This is confirmed in Fig. 7. Both quantities show an almost linear evolution with the amount of PVME in the sample. However, as the attenuation data show a lot of scatter for concentrations above 30 wt%, the most relevant information for the state diagram is obtained below 30 wt% PVME using HR-US. As less accurate information is obtained for higher concentrations, these data were not included in the graphs. The relative change in the difference ultrasonic velocity (up to 80% of the initial homogeneous value) is smaller than that in the ultrasonic attenuation (up to 500% of the initial homogeneous value), indicating that the attenuation might be more sensitive for studying phase separation. Note that these relative changes in both ultrasonic signals are considerably larger than for the PNIPAM/water system (50 and 300%, respectively) that was previously studied [4]. This dissimilarity can be understood when considering the different types of LCST demixing. That is, the shape of the type II LCST demixing curve in combination with the

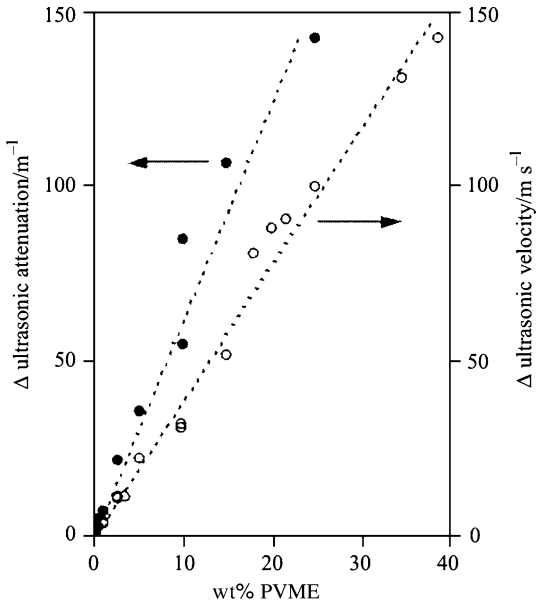

Fig. 7 Concentration-dependence of ultrasonic properties for PVME/water ($f = 7.5$–8.5 MHz): *delta* Ultrasonic velocity (*open circle*) and *delta* Ultrasonic attenuation (*filled circle*), at 35 °C

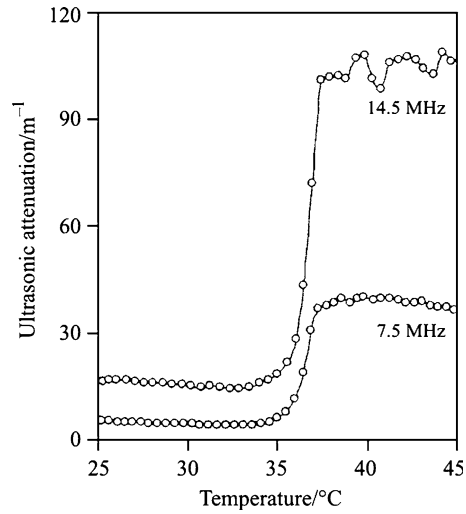

Fig. 8 Ultrasonic attenuation during non-isothermal demixing of 5/95 PVME/water for different frequencies ($f = 7.5$ and 14.6 MHz)

interference of vitrification during phase separation, limits the degree of polymer aggregation within the PNIPAM/water mixture. Hence, the arrested change in composition results in a vitrified PNIPAM-rich phase, which still contains ca. 30 wt% of water at 38.5 °C, whereas in the case of PVME/water a highly concentrated PVME-rich phase is formed (containing less than 4 wt% of water), without interference of vitrification during LCST demixing.

The ultrasonic velocity is normally frequency-independent [1, 4], while the attenuation depends on the applied frequency. Figure 8 illustrates that with increasing frequency, the ultrasonic attenuation in the homogeneous region enlarges and the change at T_{demix} becomes bigger. This frequency-dependence can be exploited to envision weak transitions, as is often the case when dealing with dilute aqueous polymer solutions. Note that the present analysis of the ultrasonic attenuation does not allow identifying a possible contribution from concentration fluctuations near the phase separation region due to the limited number of frequencies investigated. In order to clarify this issue a more elaborated frequency study is needed as was demonstrated for poly(ethylene glycol)/poly(propylene glycol) blends [14, 58]. This is, however, beyond the scope of this work.

Non-isothermal remixing

The investigated PVME/water mixtures phase separate upon heating and consequently they are expected to remix during cooling. When performing a heating/cooling cycle using HR-US, the ultrasonic attenuation curve shows some small differences between heating (Fig. 9, open circle) and cooling (Fig. 9, filled circle) in the temperature range 35–45 °C, thus indicating some variation in morphology of the aggregates upon demixing and remixing, respectively. Nevertheless, a second heating/cooling cycle is just about identical with the first one, indicating the complete reversibility of the phase separation process. Note that such examination was more difficult to perform with concentrated mixtures (i.e., with concentrations $\geq$30 wt% PVME), as the level of aggregation sometimes led to sedimentation causing a simultaneous decrease in both the velocity and the attenuation. Additionally, using MTDSC, a much smaller contribution is found in $c_{\text{p}}^{\text{app}}$ (Fig. 10, thin curves) as compared to the one upon heating (Fig. 10, thick

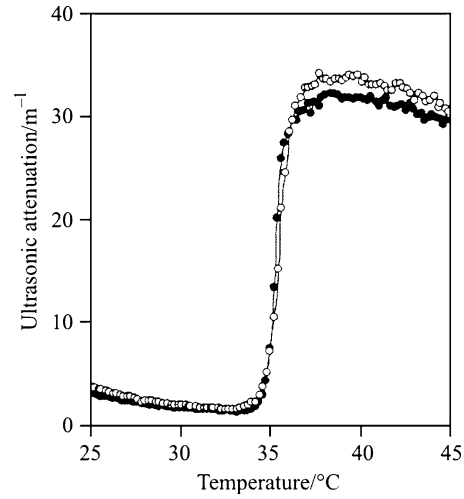

Fig. 9 Ultrasonic attenuation during non-isothermal demixing (*open circle*) and remixing (*filled circle*) of 3/97 PVME/water

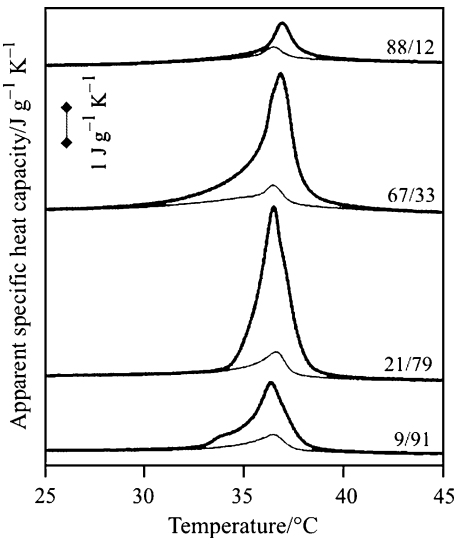

Fig. 10 Non-isothermal demixing and remixing of PVME/water for different compositions: apparent specific heat capacity (MTDSC) during demixing (heating: *thick*) and remixing (cooling: *thin*), curves are shifted vertically for clarity

curves), even though the total remixing enthalpy upon cooling nearly equals the total demixing enthalpy. The smaller contribution in c_p^{app} indicates that the characteristic time scale for remixing is longer in relation to the modulation period, i.e., the remixing process is slower than the preceding demixing [33]. As a result, the contribution of the remixing enthalpy in the non-reversing heat flow amounts up to 80% of the total heat flow and is as such significantly larger than during demixing. Hence, both techniques illustrate that for the PVME/water system the remixing upon cooling is (somewhat) slower than the demixing upon heating. These kinetic observations are most obvious for MTDSC because of its ability to measure at higher concentrations and because the balance between the separation in reversing and non-reversing contributions is very sensitive to the kinetics of the observed transformations.

Conclusions

A High Resolution Ultrasonic Resonator technique was successfully applied to study the demixing and remixing behavior of aqueous poly(vinyl methyl ether) solutions. The phase separation process causes the hydration structure surrounding the polymer chains to become gradually destroyed, which results in hydrophobic association and aggregate formation. This is seen as a decrease in the (difference) ultrasonic velocity along with an increase in the ultrasonic attenuation. The overall evolution of both ultrasonic signals reflects the ongoing compositional changes within the sample, governed by the atypical shape of the bimodal LCST demixing curve. In order to determine the demixing temperature of each composition, the (difference) ultrasonic velocity was preferred because it displays a superior signal-to-noise ratio. The invariant three-phase equilibrium could also be determined using HR-US as it causes an (additional) abrupt stepwise change in both ultrasonic signals. The HR-US data are most relevant below 30 wt% PVME as sedimentation sometimes interferes at higher concentrations.

Furthermore, HR-US provides valuable kinetic information on the phase transformations involved: the observed differences upon heating and cooling indicate that the remixing process is (somewhat) slower than the preceding demixing, as confirmed by MTDSC.

Acknowledgements The work of K. Van Durme was supported by grants from The Institute for the Promotion of Innovation through Science and Technology in Flanders (IWT-Vlaanderen). G. Van Assche is a postdoctoral fellow of the Foundation for Scientific Research (FWO-Vlaanderen). Prof. V. Buckin from the Department of Chemistry at University College Dublin (Ireland) is acknowledged for helpful discussions.

References

1. Buckin V, Smith C. Precision ultrasonic resonator measurements for analysis of liquid. Semin Food Anal. 1999;4:113–27.
2. O'Driscoll B, Smyth C, Alting AC, Visschers RW, Buckin V. Ultrasonic spectroscopy for material analysis - recent advances. Spectrosc Eur. 2003;15:20–5.
3. Buckin V, Kudryashov E, O'Driscoll B. An alternative spectroscopy technique for biopharmaceutical applications. Pharm Tech Europe. 2002;14:33–7.
4. Van Durme K, Delellio L, Kudryashov E, Buckin V, Van Mele B. Exploration of high-resolution ultrasonic spectroscopy as an analytical tool to study demixing and remixing in poly(N-isopropyl acrylamide)/water solutions. J Polym Sci B. 2005;43:1283–95.
5. Buckin VA, Kankiya BI, Sarvazyan AP, Uedaira H. Acoustical investigation of poly(da) poly(dt), poly[d(a-t)]poly[d(a-t)i, poly(a) poly(u) and DNA hydration in dilute aqueous solutions. Nucleic Acids Res. 1989;17:4189–203.
6. Buckin VA, Kankiya BI, Rentzeperis D, Marky LA. Mg^{2+} recognizes the sequence of DNA through its hydration shell. J Am Chem Soc. 1994;116:9423–9.
7. Buckin V, Kudryashov E, Morrissey S, Kapustina T, Dawson K. Do surfactants form micelles on the surface of DNA? Progr Colloid Polym Sci. 1998;110:214–9.
8. Kudryashov E, Kapustina T, Morrissey S, Buckin V, Dawson K. The compressibility of alkyltrimetylammonium bromide micelles. J Colloid Interface Sci. 1998;103:59–68.
9. Smyth C, Dawson K, Buckin V. Ultrasonic analysis of heat-induced coagulation in calcium fortified milk. Progr Colloid Polym Sci. 1999;112:221–6.
10. Smyth C, Kudryashov E, Buckin V. High-frequency shear and volume viscoelastic moduli of casein particle gel. Colloid Surf A. 2001;183–185:517–26.
11. Alig I. Ultrasonic relaxation and complex heat capacity. Thermochim Acta. 1997;305:35–49.

12. Fenner DB. Ultrasonic study of fluctuations in polystyrene solutions. J Chem Phys. 1987;87:2377–91.
13. Kaatze U, Schreiber U. Evidence of critical concentration fluctuation contributions to the ultrasonic-absorption spectrum of 2,6-dimethylpyridine water. Chem Phys Lett. 1988;148:241–4.
14. Mayer W, Hoffmann S, Meier G, Alig I. Critical fluctuations in a binary mixture of polyethylene glycol and polypropylene glycol studied by ultrasonic and light scattering experiments. Phys Rev E. 1997;55:3102–10.
15. Kroll DM, Ruhland JM. Sound-propagation in critical binary-mixtures. Phys Rev A. 1981;23:371–4.
16. Bhattacharjee JK, Ferrell RA. Dynamic scaling theory for the critical ultrasonic-attenuation in a binary-liquid. Phys Rev A. 1981;24:1643–6.
17. Ferrell RA, Bhattacharjee JK. Dynamic scaling theory of the critical attenuation and dispersion of sound in a classical fluid—the binary-liquid. Phys Rev A. 1985;31:1788–809.
18. McClements DJ. Particle sizing of food emulsions using ultrasonic spectrometry: principles, techniques and applications. In: Povey MJW, Mason TJ, editors. Ultrasound in food processing. London: Blackie Academic and Professional; 1998.
19. Gekko K, Noguchi H. Compressibility of globular-proteins in water at 25-degrees-C. J Phys Chem. 1979;83:2706–14.
20. Taulier N, Chalikian TV. Compressibility of protein transitions. Biochem Biophys Acta. 2002;1595:48–70.
21. Baillif PY, Tabellout M, Emery JR. Ultrasonic investigation of polyurethane gel forming systems. Macromolecules. 1999;32:3432–7.
22. Audebrand M, Doublier JL, Durand D, Emery JR. Investigation of gelation phenomena of some polysaccharides by ultrasonic spectroscopy. Food Hydrocolloid. 1995;9:195–203.
23. Povey MJW. Ultrasonic techniques for fluids characterization. San Diego: Academic Press; 1997.
24. Dukhin AS, Goetz PJ. Acoustic and electroacoustic spectroscopy for characterizing concentrated dispersions and emulsions. Adv Coll Interface. 2001;92:73–132.
25. Buckin VA. Hydration of nucleic bases in dilute aqueous solutions. Apparent molar adiabatic and isothermal compressibilities, apparent molar volumes and their temperature slopes at 25°C. Biophys Chem. 1988;29:283–92.
26. Buckin VA, Kankiya BI, Kazaryan RL. Hydration of nucleosides in dilute aqueous solutions—ultrasonic velocity and density measurements. Biophys Chem. 1989;34:211–23.
27. Buckin VA, Kankiya BI, Bulichov NV, Lebedev AV, Gukovsky IY, Chuprina VP, et al. Measurement of anomalously high hydration of (da) (dt) double helices in dilute solution. Nature. 1989;340:321–2.
28. Kudryashov E, Smyth C, Duffy G, Buckin V. Ultrasonic high-resolution longitudinal and shear wave measurements in food colloids: monitoring of gelation processes and detection of pathogens. Progr Colloid Polym Sci. 2000;115:287–94.
29. Horne RA, Almeida P, Day AF, Yu NT, Colloid J. Macromolecule hydration and effect of solutes on cloud point of aqueous solutions of polyvinyl methyl ether: a possible model for protein denaturation and temperature control in homeothermic animals. Interface Sci. 1971;35:77–84.
30. Spěváček J, Hanyková L, Starovoytova L. H-1 NMR relaxation study of thermotropic phase transition in poly(vinyl methyl ether)/D_2O solutions. Macromolecules. 2004;37:7710–8.
31. Guo YL, Sun BJ, Wu PY. Phase separation of poly(vinyl methyl ether) aqueous solution: a near-infrared spectroscopic study. Langmuir. 2008;24(10):5521–6.
32. Maeda H. Interaction of water with poly(vinyl methyl-ether) in aqueous-solution. J Polym Sci B. 1994;32:91–7.
33. Swier S, Van Durme K, Van Mele B. Modulated-temperature differential scanning calorimetry study of temperature-induced mixing and demixing in poly(vinylmethylether)/water. J Polym Sci B. 2003;41:1824–36.
34. Yang YY, Zeng F, Xie XL, Tong Z, Liu XX. Phase separation and network formation in poly(vinyl methyl ether)/water solutions. Polym J. 2001;33:399–403.
35. Maeda Y. IR spectroscopic study on the hydration and the phase transition of poly(vinyl methyl ether) in water. Langmuir. 2001;17:1737–42.
36. Van Durme K, Bernaerts KV, Verdonck B, Du Prez FE, Van Mele B. End-group modified poly(methyl vinyl ether): Characterization and LCST demixing behavior in water. J Polym Sci B. 2006;44:461–9.
37. Schäfer-Soenen H, Moerkerke R, Berghmans H, Koningsveld R, Dušek K, Šolc K. Zero and off-zero critical concentrations in systems containing polydisperse polymers with very high molar masses. 2. The system water–poly(vinyl methyl ether). Macromolecules. 1997;30:410–6.
38. Meeussen F, Bauwens Y, Moerkerke R, Nies E, Berghmans H. Molecular complex formation in the system poly(vinyl methyl ether)/water. Polymer. 2000;41:3737–43.
39. Shan J, Chen J, Nuopponen M, Tenhu H. Two phase transitions of poly(N-isopropylacrylamide) brushes bound to gold nanoparticles. Langmuir. 2004;20:4671–6.
40. Kujawa P, Watanabe H, Tanaka F, Winnik FM. Amphiphilic telechelic poly(N-isopropylacrylamide) in water: From micelles to gels. Eur Phys J. 2005;E17:129–37.
41. Dubovik AS, Makhaeva EE, Grinberg VY, Khokhlov AR. Energetics of cooperative transitions of N-vinylcaprolactam polymers in aqueous solutions. Macromol Chem Phys. 2005;206(9):915–28.
42. Van Durme K, Verbrugghe S, Du Prez FE, Van Mele B. Influence of poly(ethylene oxide) grafts on kinetics of LCST behavior in aqueous poly(N-vinylcaprolactam) solutions and networks studied by modulated temperature DSC. Macromolecules. 2004;37:1054–61.
43. Van Durme K, Van Assche G, Van Mele B. Kinetics of demixing and remixing in poly(N-isopropylacrylamide)/water studied by modulated temperature DSC. Macromolecules. 2004;37:9596–605.
44. Swier S, Pieters R, Van Mele B. Kinetics of demixing and remixing in poly(ethylene oxide)/poly(ether sulphone) blends as studied by modulated temperature differential scanning calorimetry. Polymer. 2002;43:3611–20.
45. Wunderlich B, Jin Y, Boller A. Mathematical-description of differential scanning calorimetry based on periodic temperature modulation. Thermochim Acta. 1994;238:277–93.
46. Reading M, Luget A, Wilson R. Modulated differential scanning calorimetry. Thermochim Acta. 1994;238:295–307.
47. Swier S, Van Mele B. Mechanistic modeling of the epoxy-amine reaction in the presence of polymeric modifiers by means of modulated temperature DSC. Macromolecules. 2003;36:4424–35.
48. Minakov AA, Schick C. Advanced AC calorimetry of polycaprolactone in melting region. Thermochim Acta. 1999;330:109–19.
49. Pyda M, Van Durme K, Wunderlich B, Van Mele B. Heat capacity of poly(vinyl methyl ether). J Polym Sci B. 2005;43:2141–53.
50. Tanaka H. Simple physical model of liquid water. J Chem Phys. 2000;112:799–809.
51. Kell GS. Density, thermal expansivity, and compressibility of liquid water from 0 degrees to 150 degrees C: correlations and tables for atmospheric-pressure and saturation reviewed and expressed on 1968 temperature scale. J Chem Eng Data. 1975;20:97–105.
52. Del Grosso VA, Mader CW. Speed of sound in pure water. J Acoust Soc Am. 1972;52:1442–6.

53. Shinyashiki N, Matsumura Y, Mashimo S, Yagihara S. Dielectric study on coupling constant of lower critical solution of poly (vinylmethylether) in water. J Chem Phys. 1996;104:6877–80.
54. Shinyashiki N, Yagihara S, Arita I, Mashimo S. Dynamics of water in a polymer matrix studied by a microwave dielectric measurement. J Chem Phys B. 1998;102:3249–51.
55. Hayashi Y, Shinyashiki N, Yagihara S. Dynamical structure of water around biopolymers investigated by microwave dielectric measurements using time domain reflectometry method. J Non-Cryst Solids. 2002;305:328–32.
56. Nies E, Ramzi A, Berghmans H, Li T, Heenan RK, King SM. Composition fluctuations, phase behavior, and complex formation in poly(vinyl methyl ether)/D_2O investigated by small-angle neutron scattering. Macromolecules. 2005;38:915–24.
57. Wang GZ, Yu F, Shang ZY, Ying Z, Hu DD. Application of ultrasonic attenuation measurements in the studies on macromolecular conformational behaviors: phase behavior of the aqueous solution of poly(vinyl methyl ether) sensitive to temperature and the modification of the behavior by using poly (acrylic acid). Chin J Chem. 2004;22:28–32.
58. Eckert S, Meier G, Alig I. Phase behaviour of mixtures of polyethylene glycol and polypropylene glycol: influence of hydrogen bond clusters on the phase diagram. Phys Chem Chem Phys. 2002;4:3743–9.